

Hadron formation and attenuation in deep inelastic lepton scattering off nuclei

T. Falter^{*}, W. Cassing, K. Gallmeister, U. Mosel

Institut fuer Theoretische Physik, Universitaet Giessen, D-35392 Giessen, Germany

Abstract

We investigate hadron formation in deep inelastic lepton scattering on N , Kr and Xe nuclei in the kinematic regime of the HERMES experiment. The elementary electron-nucleon interaction is described within the event generator PYTHIA while a full coupled-channel treatment of the final state interactions is included by means of a BUU transport model. We find a good agreement with the measured charged hadron multiplicity ratio R_M^h for N and Kr targets by accounting for the deceleration and absorption of the primarily produced particles as well as for the creation of secondary hadrons in the final state interactions.

Key words: hadron formation, hadron attenuation, deep inelastic scattering, electroproduction, nuclear reactions, meson production

PACS: 24.10.-i, 25.30.-c, 13.60.Le

Hadron production in deep inelastic lepton-nucleus scattering (DIS) offers a promising tool to study the physics of hadronization (1). The reaction of the exchanged virtual photon (energy ν , virtuality Q^2) with a bound nucleon leads to the production of several hadrons. While the primary production is determined by the fragmentation function – in medium possibly different from that in vacuo – the number of ultimately observed hadrons and their energy distribution depends also on their rescattering in the surrounding nuclear medium. Consequently, the particle spectrum of a lepton-nucleus interaction will differ from that of a reaction on a free nucleon. In order to explore such attenuation effects the HERMES collaboration has investigated the energy ν and fractional energy $z_h = E_h/\nu$ dependence of the charged hadron multiplicity

^{*} Corresponding author.

Email address: `Thomas.Falter@theo.physik.uni-giessen.de` (T. Falter).

ratio

$$R_M^h(z, \nu) = \left(\frac{N_h(z, \nu)}{N_e(\nu)} \right)_A / \left(\frac{N_h(z, \nu)}{N_e(\nu)} \right)_D \quad (1)$$

in DIS off N (2) and Kr (3) nuclei. Here $N_h(z, \nu)$ represents the number of semi-inclusive hadrons in a given (z, ν) -bin and $N_e(\nu)$ the number of deep inelastically scattered leptons in the same ν -bin. It was suggested in Ref. (2), that a phenomenological description of the R_M^h data can be achieved if the formation time, i.e. the time that elapses from the moment when the photon strikes the nucleon until the reaction products have evolved to physical hadrons, is assumed to be proportional to $(1 - z_h)\nu$ in the target rest frame. This $(1 - z_h)\nu$ dependence of the formation time τ_f is compatible with the gluon-bremsstrahlung model of Ref. (1). In the investigations of Ref. (2) any interaction of the reaction products with the remaining nucleus during this formation time has been neglected. After the formation time the hadrons could get absorbed according to their full hadronic cross section. Another interpretation of the observed R_M^h spectra – as being due to a combined effect of a rescaling of the quark fragmentation function in nuclei due to partial deconfinement as well as the absorption of the produced hadrons – has recently been given by the authors of Ref. (4). Furthermore, calculations based on a pQCD parton model (5; 6) explain the attenuation observed in the multiplicity ratio solely by partonic multiple scattering and induced gluon radiation completely neglecting any hadronic final state interactions (FSI). It has already been pointed out by the authors of Ref. (4) that a shortcoming of the existing models is the purely absorptive treatment of the FSI. We will avoid this problem by using a semi-classical coupled-channel transport model (7) which already has been employed to describe high energy photo- (8) and electroproduction (9) off nuclei.

We point out that the formation time also plays an important role in studies of ultra-relativistic heavy-ion reactions. For example, the observed quenching of high transverse momentum hadrons in $Au + Au$ reactions relative to $p + p$ collisions is often thought to be due to jet quenching in a quark gluon plasma. However, the attenuation of high p_T hadrons might at least partly be due to hadronic rescattering processes (10; 11).

Unfortunately, the average hadron formation time is not well known and the number of $\tau_f \approx 1$ fm/c as used commonly in the Bjorken estimate for the energy density (12) is nothing but an educated guess. The nonperturbative nature of this number – due to time scales of ~ 1 fm/c and hadronic size scales of 0.5–1 fm – excludes perturbative evaluation schemes; it is hard to calculate τ_f from first principles and formation times cannot be addressed in present lattice QCD simulations. One might expect that the rather successful string models (13) shed some further light on this number, since the intrinsic

time scale τ_0 for the $q-\bar{q}$ formation vertex can be related to the fragmentation function and string tension, respectively (14). However, the actual parameters employed in current transport codes are not unique, with hadron formation times ranging from 0.3–2 fm/c (15; 16), depending on the flavor, momentum and energy of the created hadrons. In fact, the rapidity and transverse mass spectra from relativistic nucleus-nucleus collisions are not very sensitive to the formation time τ_f (11). It is therefore essential to check whether these times are compatible with constraints extracted from reactions, where the collision geometry is much better under control.

To this aim the attenuation of antiprotons produced in $p + A$ reactions at the AGS energies of 12.3 GeV and 17.5 GeV has been investigated on various nuclear targets in Ref. (17) and a range of values for $\tau_f = 0.4 - 0.8$ fm/c has been extracted in comparison to the data from the E910 Collaboration (18).

In our present approach the lepton-nucleus interaction is split into two parts: 1) In the first step the virtual photon is absorbed on a bound nucleon of the target; this interaction produces a bunch of particles that in step 2) are propagated within the transport model. Coherence length effects in the entrance channel, that give rise to nuclear shadowing, are taken into account as described in Ref. (9). The virtual photon-nucleon interaction itself is simulated by the Monte Carlo generator PYTHIA v6.2 (19) which well reproduces the experimental data of Ref. (20) on a hydrogen target. Depending on whether the photon interacts directly with the nucleon or via one of its hadronic fluctuations ($\rho^0, \omega, \Phi, J/\Psi$ or a perturbative $q\bar{q}$ fluctuation) the reaction leads to the excitation of one or more hadronic strings which in our approach are assumed to fragment very rapidly into colorless prehadrons.

The time that the reaction products need to evolve to physical hadrons, i.e., the production time t_p of the prehadrons plus the time needed to build up the hadronic wave function, we denote as formation time t_f in line with the convention in transport models. For simplicity we assume that the formation time is a constant τ_f in the rest frame of each hadron and that it does not depend on the particle species. Due to time dilatation the formation time t_f in the laboratory frame is then proportional to the particle's energy

$$t_f = \gamma \cdot \tau_f = \frac{z_h \nu}{m_h} \cdot \tau_f. \quad (2)$$

The size of τ_f can be estimated by the time that the constituents of the hadrons need to travel a distance of a typical hadronic radius (0.5–0.8 fm).

To illustrate the situation shortly after the photon nucleon reaction Fig. 1 shows the excitation and fragmentation of a hadronic string in a deep inelastic scattering process. For simplicity we do not show any gluon bremsstrahlung of the struck quark in this figure. Note, however, that the possibility of such final

state gluon radiation plus subsequent $q\bar{q}$ splitting is included in the PYTHIA part of our model and leads to the creation of additional strings (19). It has been emphasized in Ref. (21) that the string propagating through the nucleus is a rather short (white) object of length ≈ 1 fm since the slow end of the string is accelerated very fast. When the primary string fragments – due to the creation of $q\bar{q}$ pairs from the vacuum – new colorless prehadrons are produced, which we propagate in space-time.

As discussed in Ref. (22) the production time t_p of these prehadrons has to be distinguished from the total formation time t_f of the final hadrons which is dilated according to Eq. (2). It has been confirmed (23) within the Lund model that the production time t_p vanishes for $z_h \rightarrow 0$ and $z_h \rightarrow 1$. In the present numerical realization of our model we first approximate this behavior by setting the production time t_p to zero for *all* prehadrons, but will also discuss the effect of a finite production time at the end of this study.

Right after the photon nucleon interaction the primary string should interact with a hadronic cross section because its transverse size is essentially that of the original nucleon. Motivated by the constituent quark model we assume that this hadronic cross section is shared by the quark/diquark at the string ends and after the fragmentation by the so called leading prehadrons that contain this quark or diquark. Our PYTHIA simulations show that in most cases the prehadrons with $z_h \approx 1$ are such leading hadrons since they contain constituents (valence- or sea-quarks) from the target nucleon or the hadronic component of the photon. They can therefore interact directly after the photon-nucleon interaction with a constant effective cross section which we denote as σ_{lead} . The cross sections of the other prehadrons, that solely contain quarks and antiquarks created from the vacuum, emerge at intermediate z_h . They are assumed to be non-interacting until t_f . This assures that the summed cross section of the complete final state right after the photon-nucleon interaction is approximately that of the original nucleon. Each time when a new hadron has formed, the summed cross section rises just like in the approach of Ref. (21). After the hadron formation time t_f by definition all hadrons interact with their full hadronic cross section σ_h . Note, that our concept of leading hadrons is in accordance with those of other transport models for high energy reactions (11; 15; 24; 25).

Since the lighter (intermediate z_h) hadrons have large formation times in the target frame (see Eq. (2)) they may escape the nucleus without being attenuated if they are non-leading. However, many ($\approx 2/3$) of the observed hadrons with intermediate z_h are not directly produced in the string fragmentation but stem from decays of the much heavier vector mesons with correspondingly shorter formation times. These vector mesons may therefore form inside the nuclear volume and thus be subjected to FSI. The effect of the FSI, finally, will depend dominantly on the nuclear geometry, i.e. the size of the

target nucleus.

In our present study the FSI are described by a coupled-channel transport model based on the Boltzmann-Uehling-Uhlenbeck (BUU) equation which describes the time evolution of the phase space density $f_i(\vec{r}, \vec{p}, t)$ of particles of type i that can interact via binary reactions. These particles involve nucleons, baryonic resonances and mesons ($\pi, \eta, \rho, K, \dots$) that are produced either in the primary reaction or during the FSI. In this work we also have to account for the prehadrons emerging from the string fragmentation. For a particle species i the BUU equation takes the form

$$\left(\frac{\partial}{\partial t} + \frac{\partial H}{\partial \vec{p}} \frac{\partial}{\partial \vec{r}} - \frac{\partial H}{\partial \vec{r}} \frac{\partial}{\partial \vec{p}} \right) f_i(\vec{r}, \vec{p}, t) = I_{coll}[f_1, \dots, f_i, \dots, f_M], \quad (3)$$

where the Hamilton function H includes a position and momentum dependent mean-field potential for baryons. The collision integral on the right hand side accounts for the creation and annihilation of particles of type i in a collision as well as elastic scattering. The transition rates are determined from the particular (vacuum) cross sections. For fermions Pauli blocking is taken into account in I_{coll} via blocking factors. The prehadrons are treated like ordinary hadrons except for their modified interaction cross section and the fact that they are not allowed to decay during the formation time. The BUU equations of each particle species i are coupled via the collision integral and the mean field in case of baryons. The resulting system of coupled differential-integral equations is solved via a test particle ansatz for the phase space density. For further details of the transport model we refer the reader to Ref. (7).

Most of the hadronic FSI happen with invariant energies $\sqrt{s} \geq 2.2$ GeV and are described within the Lund string formation and decay scheme (13) as also implemented in the transport approaches (7; 8; 9) as well as (15; 17; 24). The important difference between a purely absorptive treatment of the FSI and the coupled-channel description provided by the BUU model is that in an interaction with a nucleon a hadron might not only be absorbed or recreated but also be decelerated in an elastic or inelastic collision. Furthermore, it may in addition produce several low energy particles. In the case of electroproduction of hadrons these interactions leads to a redistribution of strength from the high z_h part of the hadron energy spectrum to lower values of the energy fraction z_h .

In our calculation we employ all kinematic cuts of the HERMES experiment as well as the geometrical cuts of the detector. In actual numbers: we require for the Bjorken scaling variable $x = \frac{Q^2}{2m_N \nu} > 0.06$ (with m_N denoting the nucleon mass), for the photon virtuality $Q^2 > 1$ GeV² and for the energy fraction of the virtual photon $y = \nu/E_{beam} < 0.85$. In addition, the PYTHIA model introduces a lower cut in the invariant mass of the photon-nucleon system at

$W = 4$ GeV that is above the experimental constraint $W > 2$ GeV. This limits our calculations to minimal photon energies of $\nu_{min} = 8.6$ GeV as compared to $\nu_{min} = 7$ GeV in the HERMES experiment and leads to a suppression of high Q^2 events at energies below $\nu \approx 15$ GeV.

In Fig. 2 we present the average values of Q^2 and $\nu(z_h)$ for our simulated event samples on N and Kr as a function of z_h (ν) in comparison to the experimental quantities (26). In order to compare with the ν dependence of $\langle Q^2 \rangle$ and $\langle z_h \rangle$ we only account for hadrons with $z_h > 0.2$ as in the HERMES experiment. For both the N and the Kr target the average kinematical variables are well reproduced by our model. The underestimation of $\langle Q^2 \rangle$ at low photon energies $\nu < 12$ GeV is due to the PYTHIA cut in $W \geq 4$ GeV which suppresses higher values of Q^2 at low photon energies ν . This is also the reason why the average value of Q^2 in the z_h spectrum comes out slightly too low within our model.

We proceed with a discussion of the actual results of our PYTHIA + BUU simulations. In Fig. 3 we show the calculated multiplicity ratio R_M^h for N and Kr targets using an 'estimated' formation time of 0.5 fm/c and different values for the leading prehadron cross section σ_{lead} . The data have been taken from Refs. (2; 3). Since the particles with z_h close to 1 are predominantly leading hadrons we can use the high z_h part in the fractional energy spectrum to obtain information on σ_{lead} . The data for both nuclei indicate that σ_{lead} has to be in the range $0-0.5 \sigma_h$ with σ_h ($h = \pi^\pm, K^\pm, p, \dots$) taken from (27). For the heavier nucleus, Kr , we clearly underestimate the hadron attenuation with $\sigma_{lead}=0$ since most of the particles, especially those with large energies, escape the nucleus due to time dilatation. If one wants to describe the strong attenuation of hadrons at large fractional energy z_h without any prehadronic interactions one would need an unphysical short formation time $\tau_f < 0.1$ fm/c. This, however, is ruled out by the measured ν dependence of R_M^h since a vanishing formation time leads to a multiplicity ratio R_M^h which is considerably too low (see dash-dotted and dash-dot-dotted curves in Fig. 4).

The dotted line in Fig. 3 shows the result of a calculation where the leading prehadrons interact with the full hadronic cross section σ_h ; this leads to a too strong attenuation of charged hadrons. A good agreement with the data is achieved for $\sigma_{lead} = 0.33\sigma_h$ during the formation time τ_f as can be seen in Fig. 4. We note, that this value for σ_{lead} represents an average value over time from the virtual photon-nucleon interaction to the actual hadron formation time. For a detailed investigation we refer the reader to a forthcoming study (28).

In Fig. 4 we investigate the influence of different formation times τ_f on R_M^h using the effective cross section $\sigma_{lead} = 0.33\sigma_h$. We find, that formation times $\tau_f \gtrsim 0.3$ fm/c are needed to describe the experimental data with little sensitivity to higher values. This is compatible to the range of values extracted from the antiproton attenuation studies in Ref. (17). The steep rise of R_M^h

for $z_h \lesssim 0.2$ is caused by the energy loss and the production of low energy secondary particles in elastic and inelastic FSI. We mention that in models dealing with purely absorptive FSI a ratio much larger than one can only be explained by a drastic change of the fragmentation function.

We note that the photon energy dependence of the ratio R_M^h for the Kr target is less well reproduced for energies below 14 GeV. The reason for this can be traced back to the $W \geq 4$ GeV cut of the PYTHIA model. Our simulations show that the number of leading hadrons decreases with Q^2 for fixed energy, but the $W \geq 4$ GeV cut discards larger values of Q^2 at energies $\nu < 15$ GeV. For higher values of Q^2 the importance of DIS events rises as compared to events, where the photon interacts via a vector meson fluctuation (VMD events). In the latter case one has initially 5 constituent quarks and antiquarks and thus gets more leading prehadrons than in a DIS event. This leads to a mismatch of leading and nonleading prehadrons in the region $z_h \lesssim 0.4$. Since the number of prehadrons created in an electron-nucleon collision decreases exponentially with increasing z_h , this region contributes dominantly to the z_h integrated ν spectrum. This deficiency of the present model will be cured in a more detailed upcoming work (28).

In the pQCD parton model of Ref. (5) the multiple parton scattering leads to a modification of the fragmentation function and predicts a hadron attenuation $\sim A^{2/3}$. In our approach, however, the fragmentation is assumed to be decided on time scales of the nucleon dimension itself such that only the 'free' fragmentation function enters. All attenuation effects then are attributed to FSI of the leading and secondary (pre-)hadrons. In order to distinguish experimentally between the different concepts, it is thus important to get the scaling with target mass A . To this aim Fig. 4 also shows predictions for a Xe target. In accordance with the authors of Ref. (4) we predict only a small change in the multiplicity spectra compared to the Kr target such that the scaling exponent is lower than $2/3$.

Finally, we discuss the effect of a finite production time t_p (in the lab frame) for prehadrons which we adopt, for consistency, from the Lund model (23):

$$t_p = \left(\frac{\ln(1/z^2) - 1 + z^2}{1 - z^2} \right) \frac{z\nu}{\kappa}. \quad (4)$$

Here $\kappa \approx 1 \text{ GeVfm}^{-1}$ denotes the string tension. In the following we assume no interaction before t_p and the full hadronic cross section for prehadrons for $t \geq t_p$, i.e., there is no dependence on the formation time t_f anymore. The dashed line in Fig. 5 represents the result of a Glauber-like treatment of the FSI where every time a prehadron interacts with another particle it is removed from the outgoing channel. As the authors of Ref. (4) we get a good description of the z -dependence of the multiplicity ratio. However, the ν spectrum is not

attenuated strongly enough at the higher ν (r.h.s. of Fig. 5). The solid curves show the effect of the coupled channels, i.e., a particle is not only absorbed in a collision but produces a bunch of low energy particles, thereby shifting strength to the low z part of the spectrum and thereby underestimating the attenuation at low z . Similarly, the attenuation is also too weak in the ν -spectrum. Since an additional formation time with reduced cross sections would further enhance these discrepancies, we conclude that the data cannot be described with the production time (4). For a detailed investigation of finite production times and alternative models we refer the reader to a forthcoming work (28).

In summary, we have shown that one can describe the experimental data of the HERMES collaboration for hadron attenuation on nuclei without invoking any changes in the fragmentation function due to gluon radiation. In our dynamical studies, that include the most relevant FSI, we employ only the 'free' fragmentation function on a nucleon and attribute the hadron attenuation to the deceleration of the produced (pre-)hadrons due to FSI in the surrounding medium. We find that in particular the z -dependence of R_M^h is very sensitive to the interaction cross section of leading prehadrons and can be used to determine σ_{lead} . The interaction of the leading prehadrons during the formation time could be interpreted as an in-medium change of the fragmentation function, which however could not be given in a closed form. The extracted average hadron formation times of $\tau_f \gtrsim 0.3$ fm/c are compatible with the analysis of antiproton attenuation in $p+A$ reactions at AGS energies (17). In an upcoming work we will investigate in detail the spectra for different particle species (π^\pm , K^\pm , p , \bar{p}) to examine, if the formation times of mesons and antibaryons are about equal. In addition we will improve our model to describe the primary photon-nucleon reaction below the PYTHIA threshold of $W \geq 4$ GeV.

The authors acknowledge valuable discussions with N. Bianchi, E. Garutti, C. Greiner, V. Muccifora and G. Van Steenhoven. This work was supported by DFG.

References

- [1] B. Kopeliovich, J. Nemchik, E. Predazzi, in: G. Ingelman, A. De Roeck, R. Klanner (Eds.), Proceedings of the workshop on Future Physics at HERA (DESY, 1995/96), vol 2, p. 1038, nucl-th/9607036.
- [2] A. Airapetian, et al., HERMES Collaboration, Eur. Phys. J. C20 (2001) 479–486.
- [3] V. Muccifora, HERMES Collaboration, Nucl. Phys. A711 (2002), 254–263; E. Garutti, HERMES Collaboration, Acta Phys. Pol. B33 (2002) 3013–3017.
- [4] A. Accardi, V. Muccifora, H.-J. Pirner, Nucl. Phys. A720 (2003) 131–156.

- [5] X. Guo, X. N. Wang, Phys. Rev. Lett. 85 (2000) 3591–3594; X. N. Wang, X. Guo, Nucl. Phys. A696 (2001) 788–832; E. Wang, X. N. Wang, Phys. Rev. Lett. 89 (2002) 162301; X. N. Wang, Nucl. Phys. A715 (2003) 775–778.
- [6] F. Arleo, Eur. Phys. J. C30 (2003) 213–221.
- [7] M. Effenberger, E. L. Bratkovskaya, U. Mosel, Phys. Rev. C60 (1999) 044614.
- [8] M. Effenberger, U. Mosel, Phys. Rev. C62 (2000) 014605; T. Falter, U. Mosel, Phys. Rev. C66 (2002) 024608.
- [9] T. Falter, K. Gallmeister, U. Mosel, Phys. Rev. C67 (2003) 054606.
- [10] K. Gallmeister, C. Greiner, Z. Xu, Phys. Rev. C67 (2003) 044905.
- [11] W. Cassing, K. Gallmeister, C. Greiner, Nucl. Phys. A735 (2004) 277–299.
- [12] J. D. Bjorken, Phys. Rev. D27 (1983) 140–151.
- [13] B. Andersson, G. Gustafson, H. Pi, Z. Phys. C57 (1993) 485–494.
- [14] B. Andersson, G. Gustafson, B. Soderberg, Z. Phys. C20 (1983) 317.
- [15] W. Cassing, E. L. Bratkovskaya, Phys. Rep. 308 (1999) 65–233.
- [16] S. Scherer, et al., Prog. Part. Nucl. Phys. 42 (1999) 279–293.
- [17] W. Cassing, E. L. Bratkovskaya, O. Hansen, Nucl. Phys. A707 (2002) 224–238.
- [18] I. Chemakin, et al., Phys. Rev. C64 (2001) 064908.
- [19] T. Sjöstrand, et al., Comput. Phys. Commun. 135 (2001) 238–259; T. Sjöstrand, L. Lönnblad, S. Mrenna, PYTHIA 6.2 Physics and Manual, hep-ph/0108264.
- [20] A. Airapetian, et al., HERMES Collaboration, Eur. Phys. J. C21 (2001) 599–606.
- [21] C. Ciofi degli Atti, B. Z. Kopeliovich, Eur. Phys. J. A17 (2003) 133–144.
- [22] B. Z. Kopeliovich, J. Nemchik, E. Predazzi, A. Hayashigaki, hep-ph/0311220.
- [23] A. Bialas, M. Gyulassy, Nucl. Phys. B291 (1987) 793–812.
- [24] J. Geiss, W. Cassing, C. Greiner, Nucl. Phys. A644 (1998) 107–138.
- [25] S. A. Bass, et al., Prog. Part. Nucl. Phys. 41 (1998) 225–370.
- [26] N. Bianchi, V. Muccifora, private communication.
- [27] K. Hagiwara, et al., PDG, Phys. Rev. D66 (2002) 010001.
- [28] T. Falter, et al., in preparation.

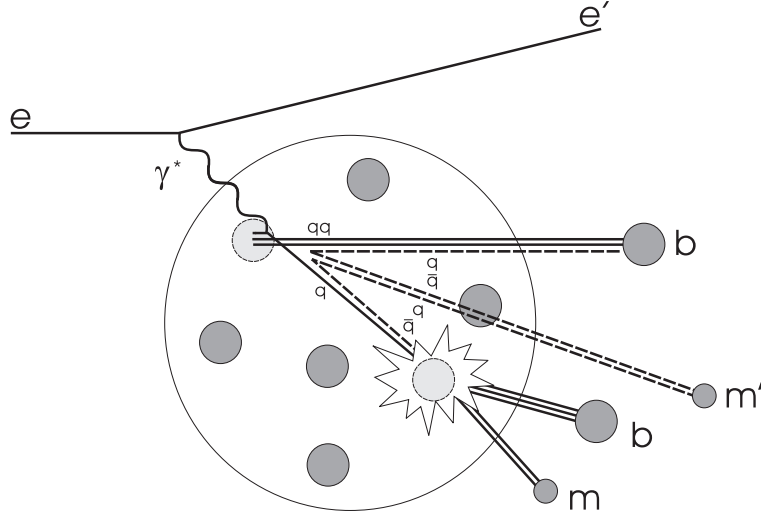


Fig. 1. Illustration of an electron nucleus interaction: The virtual photon γ^* excites a hadronic string by hitting a quark q inside a bound nucleon. In our example the string between the struck quark q and diquark qq fragments due to the creation of two quark-antiquark pairs. One of the antiquarks combines with the struck quark to form a 'leading' pre-meson m , one of the created quarks combines with the diquark to form a 'leading' pre-baryon b . The remaining partons combine to a pre-meson m' that, depending on the mass of the meson, might leave the nucleus before it hadronizes (see Eq. (2)). Note that in our approach the actual production time t_p of the non-leading prehadrons has no effect on our results since we neglect any interaction until t_f . See text for details.

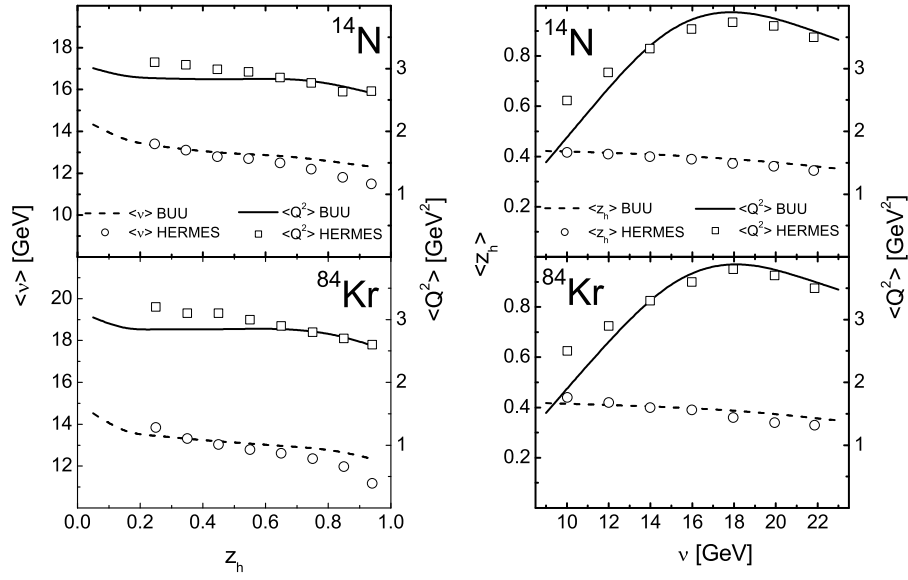


Fig. 2. Model predictions for the average values of the kinematic variables in charged hadron production in comparison with the experimental numbers at HERMES. For the calculation we used the formation time $\tau_f = 0.5$ fm/c and a leading prehadron cross section $\sigma_{\text{lead}} = 0.33\sigma_h$. *Left:* $\langle \nu \rangle$ and $\langle Q^2 \rangle$ as a function of z_h compared to the experimental values for N and Kr targets (26). *Right:* Same for $\langle z_h \rangle$ and $\langle Q^2 \rangle$ as a function of ν .

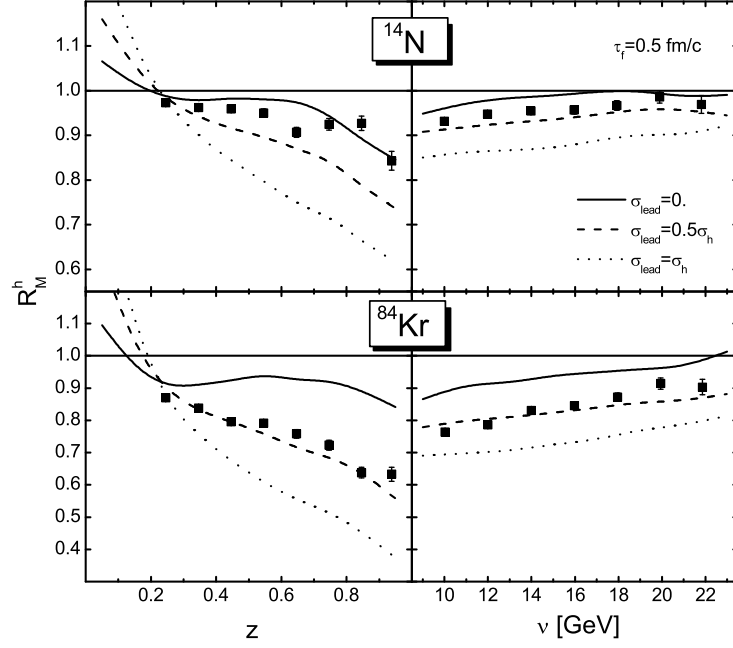


Fig. 3. Calculated multiplicity ratios (Eq. (1)) of charged hadrons for N and Kr targets for fixed formation time $\tau_f = 0.5$ fm/c and different values of the leading prehadron cross section: $\sigma_{\text{lead}} = 0.$, i.e. without any prehadronic interaction (solid line), $\sigma_{\text{lead}} = 0.5\sigma_h$ (dashed line) and $\sigma_{\text{lead}} = \sigma_h$ (dotted line). The data for the Nitrogen target have been taken from Ref. (2) while the Krypton data stem from Ref. (3).

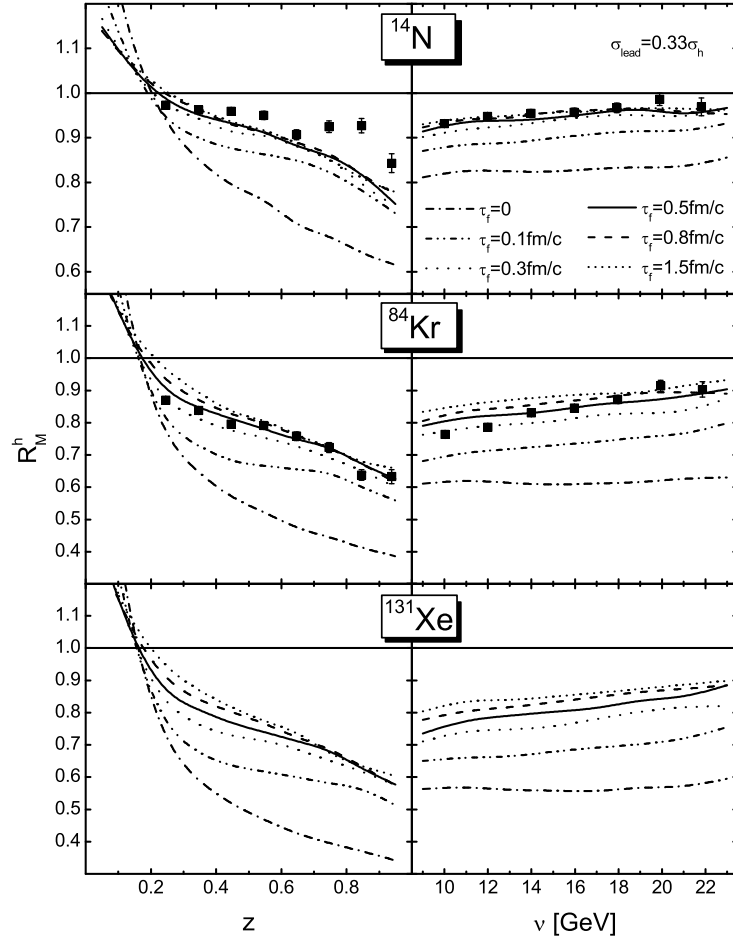


Fig. 4. Calculated multiplicity ratios of charged hadrons for N , Kr and Xe targets for a fixed leading prehadron cross section $\sigma_{\text{lead}} = 0.33\sigma_h$ and different values of the formation time from $\tau_f = 0$ to 1.5 fm/c. The data are the same as in Fig. 3.

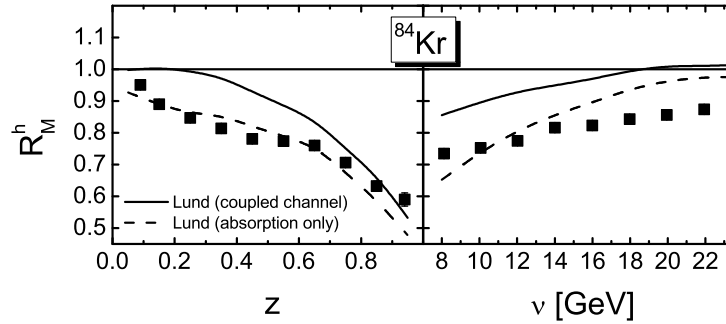


Fig. 5. Calculated multiplicity ratios of charged hadrons for a Kr target assuming the finite production time t_p given by Eq. (4). For $t \geq t_p$ the prehadrons interact with their full hadronic cross section. The dashed line shows the result of a simulation with a purely absorptive treatment of the FSI. The solid line represents the coupled-channel result.